Understanding the Elastomeric Properties of Polymer Networks

R.F.T. Stepto[*1], *J.I. Cail*[1], *D.J.R. Taylor*[1], *I.M. Ward*[2] and *R.A. Jones*[2]

[1]Polymer Science and Technology Group, Manchester Materials Science Centre, UMIST & University of Manchester, Grosvenor Street Manchester, UK M1 7HS
[2]IRC in Polymer Science and Technology, Department of Physics, University of Leeds, Leeds, UK LS2 9JT

SUMMARY: It is shown that Monte-Carlo (MC) simulations of the elastic behaviour of chains in networks using realistic rotational-isomeric-state (RIS) chain models are able to reproduce experimentally observed deviations from Gaussian network behaviour in uniaxial extension and also to interpret, quantitatively, stress-optical properties. In stress-strain behaviour, an increase in the proportion of fully extended chains with increasing macroscopic strain gives rise to a steady decrease in the rate of change of the Helmholtz energy of a network, causing a reduction in network modulus at moderate macroscopic strains. There is no need to invoke a transition from affine to phantom chain behaviour as deformation increases. To evaluate stress-optical properties, the average orientation of segments with respect to the deformation axis is calculated, taking into account the interdependence of segment orientation and chain orientation as chains become more extended and aligned under uniaxial stress. The MC method gives, in agreement with experiment, values of stress-optical coefficient that are dependent upon both deformation ratio and network-chain length. The method highlights serious shortcomings in the classical Gaussian model of stress-optical behaviour. Applications of the simulation methods to the quantitative modelling of the stress-strain behaviour of poly(dimethyl siloxane) networks and the stress-optical behaviour of polyethylene networks are described.

Introduction

Calculations of elastomeric properties of polymer networks have conventionally used theories and models based on the behaviour of a collection of "average" chains, with all the chains responding identically to external forces[1-4]. Although the molecular origin of the elastic force in a rubber-like material has long been acknowledged, the relationships between deformations at the macroscopic and molecular levels are not yet fully understood. It is thought that the initial network-chain deformation accompanying sample deformations is affine in the macroscopic strain, giving rise to the experimentally observed initial network modulus; as macroscopic deformation increases, the modulus is seen to decrease as the network chain deformation deviates from affine[1-6]. Finally, as more and more chains reach full extension, the network modulus increases rapidly (before sample rupture), due to the onset of stress-induced crystallisation, or as a result of energy changes associated with valence-angle deformation and bond stretching.

 CCC 1022-1360/00/$ 17.50+.50/0

A Monte-Carlo (MC) approach developed by the authors[5-8] has shown that the different responses of individual chains have to be accounted for in defining overall, statistical-mechanically averaged network behaviour and properties. Actual, rather than equivalent Gaussian or Langevin, network-chain end-to-end distance distributions are used. This paper describes the approach and its applications to stress-strain and stress-optical behaviour.

Stress-Strain Behaviour

The first stage in the MC simulation involves the numerical generation of the radial end-to-end distance distribution, $W(r)$, for unperturbed chains of various numbers of skeletal bonds (n) at a fixed temperature according to a rotational-isometric-state (RIS) or other realistic model. The corresponding values of probability density $P(\boldsymbol{r})$, are evaluated as $W(r)/4\pi r^2$, assuming the random orientation of chains in three dimensions. For poly(dimethyl siloxane) (PDMS)[5,6], the Flory-Crescenzi-Mark RIS model[9] was used and, for polyethylene (PE)[6], the Abe-Jernigan-Flory RIS model[10].

The second stage concerns simulation of the elastic behaviour of a network. The "network" is represented by a sample of spherically-symmetrical individual chains in a Cartesian laboratory-reference frame; one end of each chain is fixed at the origin. The chains are deformed uniaxially by a deformation ratio, λ, with $\lambda_x\lambda_y\lambda_z = 1$ (i.e. constancy of volume). The end-to-end distances are allowed to increase only up to their effective, conformational maximum, r_{max}^*, above which $W(r) = 0$ according to the sampled $W(r)$. For an individual polymer chain, in a network of N chains, the Helmholtz energy change upon deformation at an absolute temperature T, is assumed to arise solely from the corresponding entropic change. Hence,

$$\Delta A / NkT = \ln\{P(\boldsymbol{r}_o) / P(\boldsymbol{r}_{def})\} \quad , \tag{1}$$

where the subscripts "o" and "def" denote the relaxed and deformed end-to-end vectors, respectively.

In the MC scheme, a chain with end-to-end distance r_o, is first chosen, in proportion to $W(r_o)$. The X- and Y- coordinates of its "free" chain-end are chosen randomly, and the Z-component defined consistent with $\boldsymbol{r}_o$. Uniaxial deformations, using a series of values of λ are applied in the Z-direction (i.e. $\lambda = \lambda_z$) and the deformed end-to-end distances calculated by simple geometry, with $\lambda_x = \lambda_y = 1/\sqrt{\lambda}$. Any values of r_{def} in excess of r_{max}^* are put equal to r_{max}^*, thus limiting r to the range of values determined by the bond-conformational energies

and consistent with $W(r)$. The associated value of $W(r_{def})$ is ascertained, and hence $\ln P(\boldsymbol{r}_{def})$ evaluated as before. The Helmholtz energy change is evaluated via equation (1), and the average change per chain at each λ calculated as

$$\Delta A / NkT = \frac{1}{N}\sum_{i=1}^{N} \ln\{P(\boldsymbol{r}_o)/P(\boldsymbol{r}_{def})\} \quad , \tag{2}$$

where N is the number of chains in the M-C sample. Typically, $N = 5 \times 10^6$.

Analysis of Results

Chain behaviour in uniaxial extension and compression may be compared by defining λ^* (< 1), the *conjugate* uniaxial compression ratio that produces the same value of $< r_{def}^2 >$ as λ, the uniaxial extension ratio. For affine chain deformation at constant volume

$$< r_{def}^2 >= (< r_0^2 > /3)(\lambda_x^2 + \lambda_y^2 + \lambda_z^2) = (< r_0^2 > /3)(\lambda^2 + 2/\lambda). \tag{3}$$

If $\lambda > 1$, then the roots of equation (3) show that

$$\lambda^* = \lambda/2\{(1 + 8/\lambda^3)^{1/2} - 1\} \tag{4}$$

will produce the same value of $< r_{def}^2 >$.

The network Helmholtz energy change can be expressed as

$$\Delta A / NkT = s(\lambda^2 + 2/\lambda - 3) \tag{5}$$

For so-called Gaussian networks, with affine chain deformation[1,2], a plot of $\Delta A/NkT$ versus $\lambda^2 + 2/\lambda - 3$ is linear, with $s = ½$. In general, s will be a function of λ and the corresponding normalised stress per unit *unstrained* cross-sectional area is[5,6]

$$\frac{\sigma}{RT\rho} = \frac{1}{M_c}\left\{2s(\lambda - 1/\lambda^2) + (\lambda^2 + 2/\lambda - 3)\frac{\mathrm{d}s}{\mathrm{d}\lambda}\right\} . \tag{6}$$

The values of s and $(\lambda^2 + 2/\lambda - 3)\mathrm{d}s/\mathrm{d}\lambda$ effectively describe the deviation of the simulated elastic behaviour from that of a bulk Gaussian network (with the same M_c), for which $s = ½$, $\mathrm{d}s/\mathrm{d}\lambda = 0$ and $\sigma = (\rho RT/M_c)(\lambda - 1/\lambda^2)$.

Theoretical Results and Discussion

The dependence of $\Delta A/NkT$ on $\lambda^2 + 2/\lambda - 3$ is illustrated in Fig. 1 for networks of PDMS chains of various lengths. The earlier departure from affine, Gaussian behaviour in uniaxial

extension compared with compression is apparent. The results also show that $s \rightarrow ½$ with increasing network chain length, as expected.

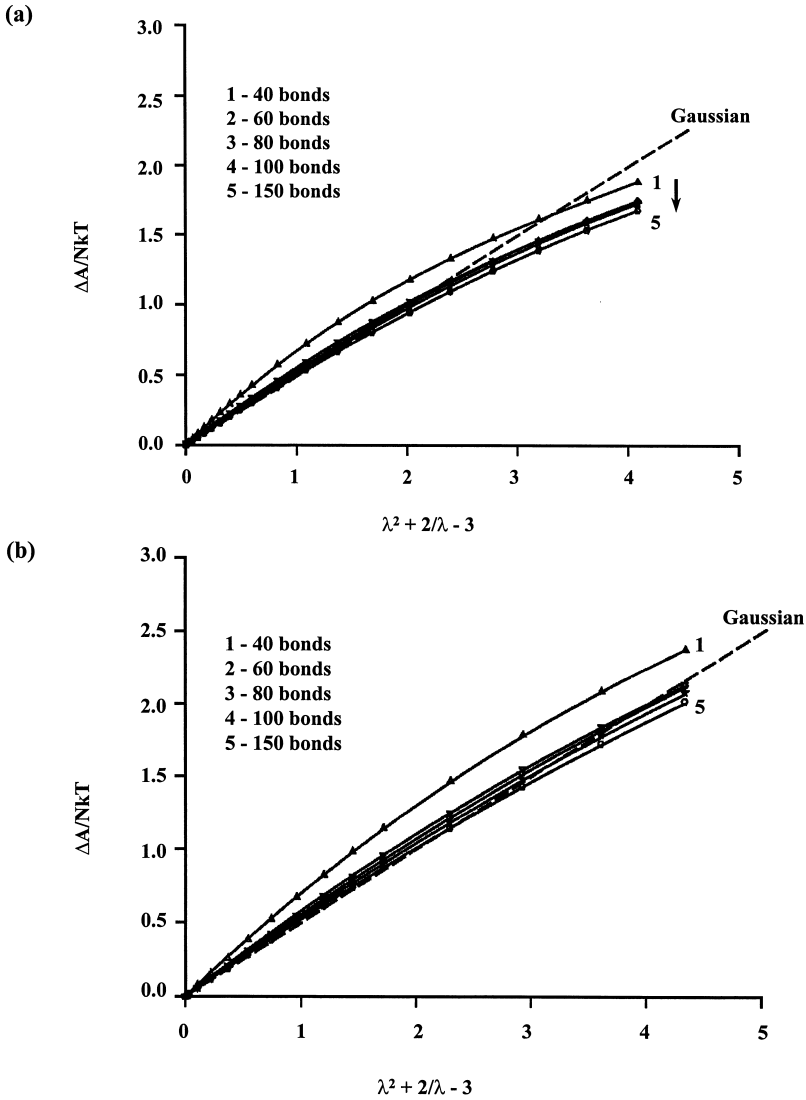

Fig. 1: Helmholtz energy change as a function of $\lambda^2 + 2/\lambda - 3$ for PDMS chains of various numbers of skeletal bonds (n) at 298K; (a) in uniaxial network extension with $\lambda = 1$ to 2.5 and (b) in uniaxial network compression with $\lambda = 1$ to 0.16.

The normalised stress, $\sigma/RT\rho$, may be calculated using equation (6), in conjunction with the values of s and $ds/d\lambda$, evaluated from the first and second derivatives of the plots in Figs. 1(a) and (b). It may then be converted to normalised reduced stress, $[\sigma^*]/RT\rho$, where

$$[\sigma^*] = \frac{\sigma}{\lambda - 1/\lambda^2} \quad . \tag{7}$$

Conventionally, the effects of non-Gaussian, non-affine behaviour are represented as positive slopes of the so-called Mooney-Rivlin plots, $[\sigma^*]$ versus $1/\lambda$ (see[4]).

Correlation with Experimental Data on PDMS Networks

The simulated PDMS-network stress-strain data are compared[5] in Fig. 2 with the experimental results of Erman and Flory[3]. These authors prepared crosslinked PDMS networks, and subjected them to uniaxial extension at various degrees of swelling in dodecane, at approximately 293K. The experimental values of $[\sigma^*]$ were normalised over $\phi_2^{1/3}$ (where ϕ_2 is the volume fraction of polymer in the swollen network) to give equivalent, dry-network behaviour. The MC data were transformed to a series of plots of $[\sigma^*]/RT\rho$ versus $1/n$ at constant $1/\lambda$. Simulated values of $[\sigma^*]$ were equated with experimental values of $[\sigma^*]/\phi_2^{1/3}$ at a reciprocal extension of $1/\lambda = 0.9$, to define an effective MC chain length, n_{M-C}, for each set of experimental results. Note, from the values in Fig. 2, that, apart from the most highly swollen network, $n_{M-C} \approx 310$ bonds to within ±2.5%. The fixing of n_{M-C} is equivalent to choosing the value of the initial modulus or M_c. Having thus established n_{M-C}, the simulated Mooney-Rivlin curve can be determined from the variation of $[\sigma^*]/RT\rho$ with $1/\lambda$ at that value of n_{M-C}. The results in Figs. 2(a) and 2(b) show that the simulated stress-strain behaviour provides a satisfactory representation of the experimental data.

Stress-Optical Behaviour: Segmental Orientation and Chain Extension

The first stage of the modelling procedure involves the calculation, of the average segment angle, ξ, relative to the chain end-to-end vector ($\boldsymbol{r}$), for an individual chain as a function of chain extension. The example of PE[7,8] is considered here. The work is also presently being extended to poly(ethylene terephthalate)[11]. For each conformation sampled using the MC scheme, the orientations of individual -CH_2- segment vectors, relative to the chain vector, are calculated. The segment vector, shown in Fig. 3(a), is defined as the vector passing through the

skeletal C atom in a direction parallel to the chain axis of an all-*trans* chain. More specifically, the vector for the i^{th} segment lies in the plane of the i^{th} and $(i\text{-}1)^{th}$ skeletal bonds, and at 34° to both bonds (since the C-C-C valence-angle supplement, $\theta = 68°$ for PE[10]). Therefore, a chain of n+1 segments (n skeletal bonds) is described in terms of n-1 segment vectors ($i = 2$ to $i = n$) and the average bond orientation for a given magnitude of end-to-end distance (r) is

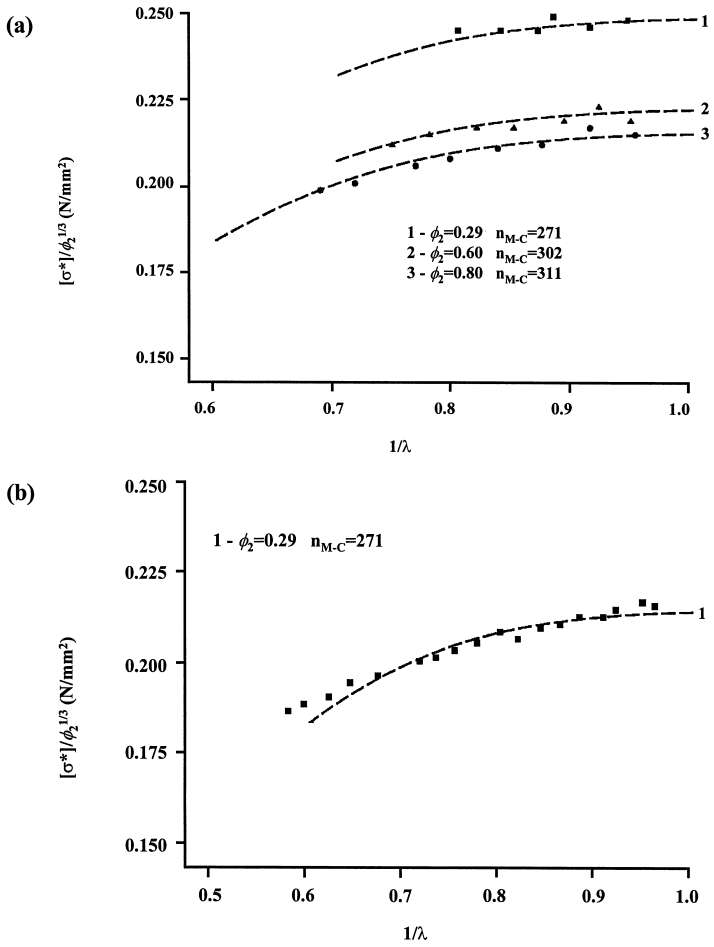

Fig. 2: MC Mooney-Rivlin curves fitted[5] to experimental data[3]; (a) networks swollen in dodecane, (b) dry network. T = 293K, density of dry network = 974 kg m^{-3}. φ_2 = network volume fraction; $n_{M\text{-}C}$ = number of bonds in MC chains required to fit $[\sigma^*]/RT\rho$ at $1/\lambda \approx 0.9$.

expressed using the average orientation function, $\langle P_2(\xi)\rangle = \frac{1}{2}(3\langle\cos^2\xi\rangle - 1)$. $\langle P_2(\xi)\rangle$ is evaluated as a function of r/r_{max} for a given value of n.

The network is subsequently represented by an array of individual PE chains, initially randomly oriented in three dimensions. It is deformed uniaxially as in the stress-strain simulations of the previous section. The resulting changes in the $<P_2(\xi)>$ function for each chain, i, are calculated to give $<P_2(\xi)>_i$. The associated changes in end-to-end vector orientation relative to the uniaxial strain direction, ψ (see Fig. 3(b)), and hence the orientation function, $P_2(\psi)$, are also calculated. The average bond orientation, $<P_2(\zeta)>$,over all chains i

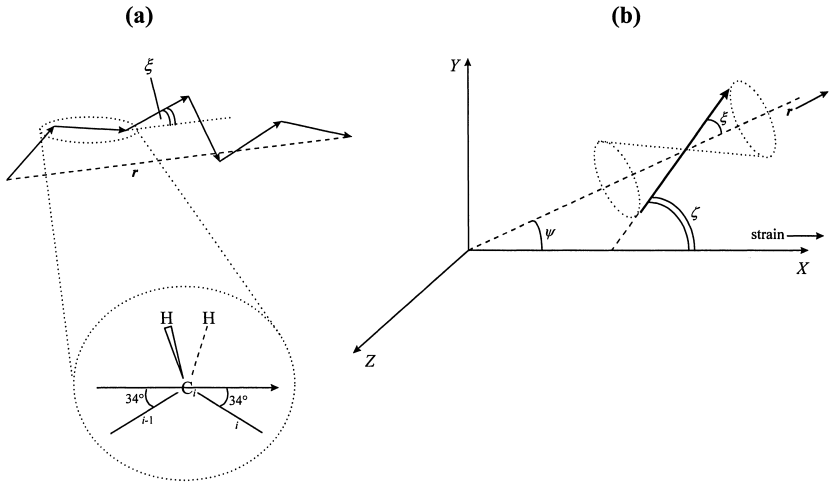

Fig. 3: (a) Illustration of the orientation angle ξ between a segment vector and the chain vector, $\boldsymbol{r}$. (b) Illustration of orientation angles: ξ, between a segment vector and chain vector, $\boldsymbol{r}$; ψ, between $\boldsymbol{r}$ and the uniaxial strain direction; and ζ, the effective angle between a segment vector and the strain direction. The segment is assumed to randomly occupy all positions on the cone defined by ξ, so that the calculated value of $P_2(\zeta)$ is an average, sampled over all cone positions of ξ.

in the MC sample, relative to the uniaxial strain direction, is calculated using the Legendre addition theorem, giving

$$<P_2(\zeta)>=<<P_2(\xi)>_i \cdot P_2(\psi_i)> \quad . \tag{8}$$

$<P_2(\zeta)>$ is also evaluated using the limiting approximation

$$<P_2(\zeta)>=<<P_2(\xi)>_i>\cdot<P_2(\psi_i)> \quad , \tag{9}$$

assuming that the average orientation functions $<<P_2(\xi)>_i>$ and $<P_2(\psi_i)>$, over the MC sample of i chains, are independent. This is true only in the zero-deformation limit ($\lambda \rightarrow 1$).

MC Simulation of Network Stress-Orientation Behaviour

The stress-strain behaviour is analysed according to equation (6), recast to give the normalised, true stress, $t/RT\rho$,

$$\frac{t}{RT\rho} = \frac{1}{nM_o}\left\{2s(\lambda^2 - \frac{1}{\lambda}) + (\lambda^3 - 3\lambda + 2)\frac{ds}{d\lambda}\right\} \quad . \tag{10}$$

M_0 is the average molar mass per skeletal bond, such that $M_c = nM_0$.

For a given value of λ, concurrently with each chain-deformation, the orientation function of the i^{th} chain vector with respect to the applied strain, denoted $P_2(\psi_i)$, is calculated[7,8]. Next, the value of $<P_2(\xi)>_i$, for the average segment orientation with respect to the direction of the i^{th} chain vector is taken as equal to the value of $<P_2(\xi)>$ at the value of r/r_{max} corresponding to the given λ for the particular chain. In the event of a chain vector being extended beyond r^*_{max}, the magnitude of the deformed vector was set equal to r^*_{max}, thus defining the maximum value of $<P_2(\xi)>_i$. However, the direction of the chain vector is allowed to rotate from the undeformed direction defined by (x_o, y_o, z_o) to that which would be defined by the affinely deformed chain, irrespective of the magnitude of r.

For the MC sample of N chains, the average chain-vector orientation with respect to the deformation axis, $< P_2(\psi_i) >$, the average segment orientation, $<< P_2(\xi)>_i>$, with respect to the end-to-end vector, and the average segment orientation with respect to the deformation axis, $<P_2(\zeta)>$, are formed, as a function of λ, using

$$< P_2(\psi_i) >= \frac{1}{N}\sum_{i=1}^{N} P_2(\psi_i) \ , \tag{11}$$

$$<< P_2(\xi) >_i >= \frac{1}{N}\sum_{i=1}^{N} < P_2(\xi) >_i \tag{12}$$

and $$< P_2(\zeta) >=<< P_2(\xi) >_i \cdot P_2(\psi_i) >= \frac{1}{N}\sum_{i=1}^{N} < P_2(\xi) >_i \cdot P_2(\psi_i) \ . \tag{13}$$

Equation (13) gives values of $<P_2(\zeta)>$ corresponding to equation (8), whereas the product of $<< P_2(\xi)>_i>$ and $<P_2(\psi_i)>$ defined by equations (11) and (12) give $<P_2(\zeta)>$ corresponding to equation (9).

The effects of using the values of $<P_2(\zeta)>$ from equations (8) and (9) on stress-orientation behaviour are shown in Fig. 4 for 40- and 220-bond PE chains. Points are plotted corresponding to intervals of 0.01 in λ. Near the origin, the plots for a given chain length, using the two averaging procedures, are indistinguishable. As macroscopic deformation increases, the larger values of $<P_2(\zeta)>$ at a given r/r_{max}, resulting from the averaging procedure of equation (8), give increases in the stress-orientation relative to that calculated from equation (9). Also, a marked non-linear behaviour is observed. The classical Gaussian approximation for $<P_2(\zeta)>$ is defined by[7)]

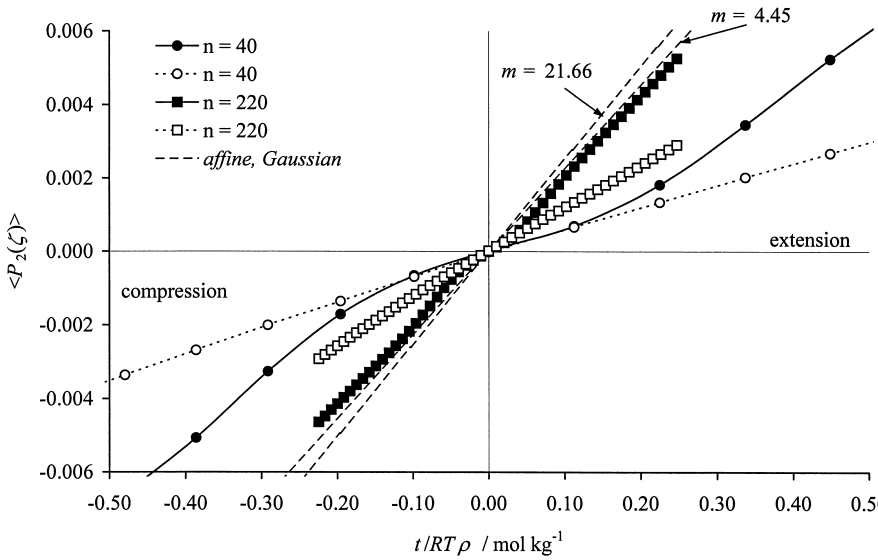

Fig. 4: $<P_2(\zeta)>$ versus normalised true stress, $t/RT\rho$, for networks of 40- and 220-bond PE chains at 403K at macroscopic extensions in the region $\lambda \rightarrow 1$, using a deformation step $\Delta\lambda = 0.01$. Closed symbols, $<P_2(\zeta)>$ evaluated according to equation (8); open symbols, $<P_2(\zeta)>$ evaluated according to equation (9). The plots for Gaussian networks of chains with $m = 4.45$ and $m = 21.66$, equivalent to the PE chains of 40 and 220 bonds are also shown.

$$< P_2(\zeta) >= \frac{M_o}{5} \cdot \frac{n}{m} \cdot \left(\frac{t}{\rho RT} \right) , \qquad (14)$$

where m is the number of freely-jointed links equivalent to n actual bonds. It gives values of orientation that are too high and show only a weak chain-length dependence, coming merely from the variation of n/m with chain length.

In Fig. 4, the linear plots from the Gaussian approximation have slopes equal to the stress-orientation coefficient[7,8], $Z_t = (M_o/5)\cdot(n/m)$. For $<P_2(\zeta)>$ based on equation (9), there is no change in slope over the range of values of λ used, although changes do occur at larger deformations[8]. The slopes on the basis of $<P_2(\zeta)>$ from equation (8) increase with extension, as λ or t increases. Hence, one needs to define Z_t based on initial slopes, namely,

$$Z_t = \left[\frac{< P_2(\zeta) > \rho RT}{t}\right]_{\lambda\to 1} . \tag{15}$$

If linear behaviour is assumed between $t = 0$ or $\lambda = 1$ and a given value of t or λ, then the *effective* value of Z_t so defined will increase initially as the given value of t increases from 0 or λ increases from 1. Further, it will, over the ranges of λ used in Fig. 4, tend to an *approximately* constant value[8], equal to about 1.77 times the value as $\lambda\to 1$. The origin of the increase is the marked orientation of segments as chains start to deform.

Experimentally, Z_t is conventionally evaluated from the measured stress-optical coefficient (C) using the equation

$$Z_t = \frac{C\rho RT}{\Delta\tilde{n}_{\max}} \quad , \tag{16}$$

where $\Delta\tilde{n}_{\max}$ is the maximum possible birefringence with all segments aligned with the macroscopic strain direction. C is formally evaluated as

$$C = \left[\frac{\Delta\tilde{n}}{t}\right]_{\lambda\to 1} , \tag{17}$$

where $\Delta\tilde{n}$ is the observed birefringence. Values of Z_t derived from the results of Saunders[12] for PE are shown in Fig. 5. The values of C came from *linear* birefringence ($\Delta\tilde{n}$) versus stress(t) plots and corresponded to $1.1 \geq \lambda \geq 1.05$ as the *smallest* deformation. Hence, the values of Z_t deduced from experimental values of C, namely C_{expt}, (corresponding to linear behaviour of $<P_2(\zeta)>$ versus $t/RT\rho$ up to $\lambda = 1.1$ to 1.2) will be about 1.77 times larger than the true limiting values as $\lambda \to 1$. That is, the true value of Z_t is given by

$$Z_t = \frac{C_{\text{expt}}\rho RT}{1.77\Delta\tilde{n}_{\text{max}}} \quad . \tag{18}$$

Thus, in Fig. 5, agreement between experiment and theory is achieved using a value of $\Delta\tilde{n}_{\text{max}}$ of 0.223, calculated using Denbigh's[13] polarisabilities based on data for gaseous CH_4 and C_2H_6, with

$$Z_t = \frac{C_{\text{expt}}\rho RT}{1.77 \times 0.223} = \frac{C_{\text{expt}}\rho RT}{0.395} \quad . \tag{19}$$

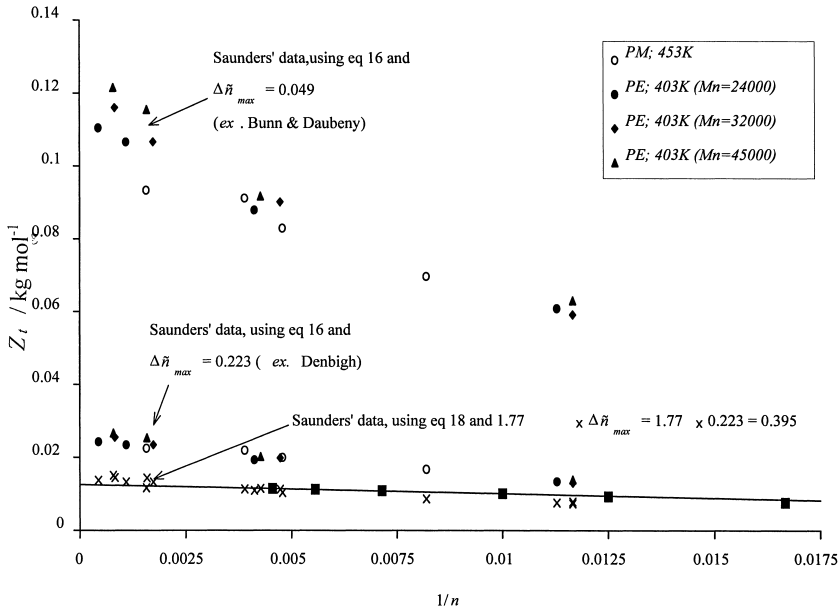

Fig. 5: Z_t versus $1/n$ calculated for model networks of 40-bond to 220-bond PE chains (■), compared with values of Z_t derived from Saunders' experimental values of the stress-optical coefficient using equation (16) with $\Delta\tilde{n}_{max} = 0.049$ (Bunn and Daubeny[14]), and $\Delta\tilde{n}_{max} = 0.223$ (Denbigh[13]), and equation (18) with $1.77 \times \Delta\tilde{n}_{max} = 1.77 \times 0.223 = 0.395$.

(The value of $\Delta\tilde{n}_{\text{max}}$ of 0.223 may be compared with a value of 0.049 calculated on the basis of Bunn and Daubeny's[14] experimental measurements of paraffin crystals. The results obtained for Z_t using $\Delta\tilde{n}_{\text{max}} = 0.049$ are also shown in Fig. 5.)

Conclusions

The described M-C network simulations using chains limited to their natural, conformational full extension is able to reproduce experimentally-observed deviations from affine, Gaussian network-chain behaviour at moderate uniaxial deformations. The concepts of a phantom network and junction-point fluctuations are not required. Decreases in the rate of Helmholtz energy change with deformation of the network occurs naturally as an increasing proportion of network chains becomes fully-extended. Further avenues of investigation still need to be explored. For example, as chains reach full extension, the contributions of valence-angle distortion and bond stretching to the network free-energy change can easily be calculated using the present approach. The predictions of the model for other modes of deformation should also be examined against experiment.

The extension of the MC simulations to the detailed modelling of stress-optical behaviour has provided the quantitative interpretation of the measured stress-optical coefficient of PE, resolving a long-standing discrepancy between theory and experiment. The approach gives, in agreement with experiment, values of C that are dependent upon both deformation ratio, λ, and network-chain length. Furthermore, the method shows that the classical, equivalent freely-jointed chain approach markedly overestimates limiting segemental orientation. There are important technological implications arising from the realistic analysis presented. For example, tensile-drawing behaviour, used in the production of fibres and films, is often understood in terms of the stretching of the molecular network, whose junction points are formed by molecular entanglements. Calculation of the maximum draw ratio achievable and, hence, the enhancement of physical properties such as modulus and strength, can now be more accurately related to measured stress-optical properties.

References

1. L.R.G. Treloar, *The Physics of Rubber Elasticity, 3rd ed.*, Oxford University Press, Oxford 1975
2. P.J. Flory, *Proc. Roy. Soc. London, Ser. A* **351**, 351 (1976)
3. B. Erman and P.J. Flory, *Macromolecules* **16**, 1607 (1983)
4. J.E. Mark and B. Erman, in: *Polymer Networks – Principles of their Formation Structure and Properties*, ed. R.F.T. Stepto, Blackie Academic & Professional, London 1998, Chapter 7
5. R.F.T. Stepto and D.J.R.Taylor, *Macromol. Symp.* **93**, 261 (1995)
6. R.F.T. Stepto and D.J.R.Taylor, *J. Chem. Soc., Faraday Trans.* **91**, 2639 (1995)
7. D.J.R. Taylor, R.F.T. Stepto, R.A. Jones and I.M. Ward, *Macromolecules* **32**,1978 (1999)

8. J.I. Cail, D.J.R. Taylor, R.F.T. Stepto, M.G. Brereton, R.A. Jones, M.E. Ries and I.M. Ward, *Macromolecules* **33**, 4966 (2000)
9. P.J. Flory, V. Crescenzi and J.E. Mark, *J. Am. Chem. Soc.* **86**, 146 (1964)
10. A. Abe, R. L. Jernigan and P. J. Flory, *J. Am. Chem. Soc.* **88**, 631 (1966)
11. I.M. Ward, M. Bleackley,D.J.R. Taylor, J.I. Cail and R.F.T. Stepto, *Polym. Engg. Sci.* **39,** 2235 (1999)
12. D.W. Saunders, *Trans. Faraday Soc.* **52**, 1425 (1956)
13. K.G. Denbigh, *Trans. Faraday Soc.* **36**, 936 (1940)
14. C.W. Bunn and R. de P. Daubeny, *Trans. Faraday Soc.* **50**, 1173 (1954)